

# Room temperature mid-infrared surface-emitting photonic crystal laser on silicon

Binbin Weng,<sup>1,a)</sup> Jiangang Ma,<sup>2</sup> Lai Wei,<sup>3</sup> Lin Li,<sup>1</sup> Jijun Qiu,<sup>1,4</sup> Jian Xu,<sup>3</sup> and Zhisheng Shi<sup>1,b)</sup>

<sup>1</sup>*School of Electrical and Computer Engineering, University of Oklahoma, Norman, Oklahoma 73019, USA*

<sup>2</sup>*School of Physics, Northeast Normal University, Changchun, Jilin 130024, China*

<sup>3</sup>*Department of Engineering Science and Mechanics, Pennsylvania State University, University Park, Pennsylvania 16802, USA*

<sup>4</sup>*State Key Laboratory of High Performance Ceramics and Superfine Microstructures, Shanghai Institute of Ceramics, Chinese Academy of Sciences, Shanghai 200050, China*

(Received 17 August 2011; accepted 13 November 2011; published online 1 December 2011)

We demonstrate a mid-infrared surface-emitting photonic crystal laser on silicon substrate operating at room temperature. The active region consisting of PbSe/PbSrSe multiple quantum wells was grown by molecular beam epitaxy on Si(111) substrate patterned with a photonic crystal (PC) array. The PC array forms a transverse magnetic polarized photonic bandgap at around  $2840\text{ cm}^{-1}$ . Under pulsed optical pumping, room temperature multimode lasing emissions were observed at wavelength  $\sim 3.5\text{ }\mu\text{m}$  with estimated threshold peak pumping intensity of  $24\text{ kW/cm}^2$ . Angular-dependent measurement indicates the lasing is of a Gaussian-like profile with full width at half maximum of  $4.66^\circ$ . © 2011 American Institute of Physics. [doi:10.1063/1.3665402]

Surface emitting photonic crystal (PC) semiconductor lasers exhibit attractive properties such as low threshold operation, circular beam with low divergence, and simplicity of monolithic integration in two-dimensional (2D) array. 2D PC semiconductor lasers have been developed rapidly in near infrared (IR) region.<sup>1-3</sup> However, mainly due to high etch-induced non-radiative surface recombination, PC semiconductor lasers in mid-infrared (mid-IR) range only achieved limited progress. For example, a pulsed electrically pumped mid-IR quantum cascade (QC) PC laser operated at 10 K was reported in 2003.<sup>4</sup> A surface-emitting PC distributed-feedback laser operated up to 180 K was demonstrated under pulsed optical pumping in 2006.<sup>5</sup> Recently, our group proposed a method to grow laser structure on Si substrate patterned with PC structure to alleviate surface recombination and demonstrated Si-based PC light emitter around  $4.3\text{ }\mu\text{m}$  with the peak power of about 4 W at 100 K and the operation temperature up to 270 K under pulsed optical pumping.<sup>6</sup> Up to date, however, mid-IR surface-emitting PC semiconductor laser operating at room temperature has not been realized yet.

In this letter, we report room temperature operation of a surface-emitting PC laser in mid-IR range on Si substrate.

In our previously reported PC light emitter work,<sup>6</sup> the 2D PC array was designed to form photonic bandgaps around 1960 and  $2300\text{ cm}^{-1}$ . These designed PC bandgaps, aligning with the gain peak of a PbSe/PbSrSe quantum well (QW) at cryogenic temperature, allow easy proof-of-concept experimental demonstration of PC modulation effect. In order to achieve room temperature PC-modulated mode emission, in this work, we constructed a 2D hexagonal holes array to form a transverse magnetic (TM) polarized photonic bandgap at around  $3.79\text{ }\mu\text{m}$  ( $\sim 2640\text{ cm}^{-1}$ ), which aligns with the room temperature gain peak of a (9.5 nm/25 nm) PbSe/

PbSrSe QW. Calculated band diagram with inter-hole spacing  $a = 2.5\text{ }\mu\text{m}$  and hole radius  $R = 1.10\text{ }\mu\text{m}$  is shown in Figure 1(a).

In the experiment, the central area of a  $1 \times 1\text{ mm}^2$  Si(111) substrate was patterned by a  $1 \times 1\text{ mm}^2$  hexagonal PC holes-array by using electron-beam (E-beam) lithography. There was only one PC defect cavity created by removing a single hole in the middle of the PC pattern. Compared to the  $7 \times 7$  defect cavities in our previous work,<sup>6</sup> single defect cavity in this work eliminates spectrum linewidth broadening caused by processing inhomogeneity of multiple PC cavities. E-Beam patterned Si substrate was then dry-etched with etching depth of  $3\text{ }\mu\text{m}$  by using a deep reactive ion etching (RIE) system. Epitaxial layers were later grown on the patterned Si by a two-chamber MBE system. The MBE growth conditions are similar to our previous report.<sup>6</sup> The epitaxial structure in this work consists of a 9-pair multiple quantum wells (MQWs) (9.5 nm PbSe/25 nm  $\text{Pb}_{0.96}\text{Sr}_{0.04}\text{Se}$ , 0.04 is the beam flux ratio of Sr and PbSe) sandwiched between a 231 nm thick  $\text{Pb}_{0.96}\text{Sr}_{0.04}\text{Se}$  bottom layer and a 25 nm thick  $\text{Pb}_{0.96}\text{Sr}_{0.04}\text{Se}$  top barrier layers; A 140 nm  $\text{BaF}_2$  capping layer was then grown on top of the epitaxial structure as the final layer of passivation and optical confinement. Figure 1(b) shows a top-view scanning electron microscopy (SEM) image of patterned area with the microcavity on Si substrate after MBE growth.

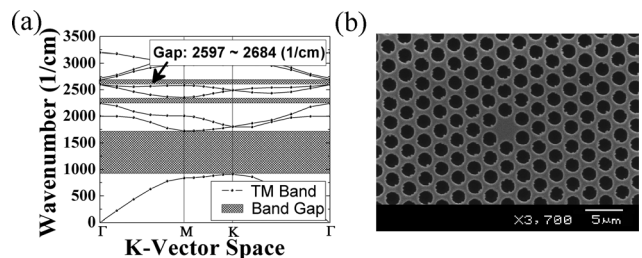


FIG. 1. (a) TM modes dispersion diagram of the 2D hexagonal photonic crystal array and (b) top-view SEM image of PbSe/PbSrSe MQWs structure grown on patterned Si (111).

<sup>a)</sup>Electronic mail: binbinweng@ou.edu.

<sup>b)</sup>Electronic mail: shi@ou.edu.

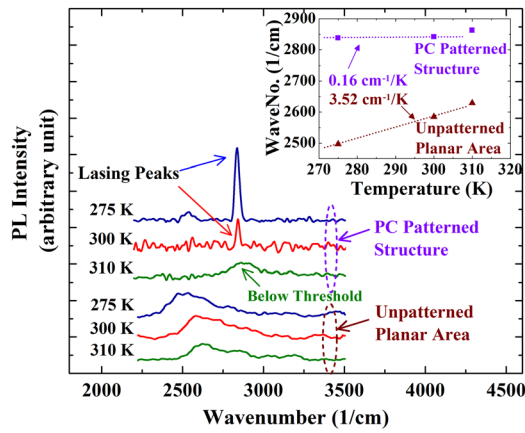


FIG. 2. (Color online) Temperature dependent light emissions of PbSe/PbSrSe MQWs on the PC patterned Si (upper group marked by dashed circle) and on un-patterned Si of the same sample (lower group marked by dashed circle). The temperature coefficients extracted from linear fits of both PC patterned and un-patterned area are shown in the inset.

Emission spectra of the as-grown sample were measured by a Fourier transform infrared (FTIR) spectrometer in step-scan mode with a  $1.064 \mu\text{m}$  pulsed pumping laser ( $\tau = 20 \text{ ns}$ ,  $10 \text{ Hz}$ ). The optical signal was detected by a liquid  $\text{N}_2$  cooled InSb detector (Judson J-10D). Within the temperature range of 275 K–310 K, there is only one emission peak from the PC patterned area of the sample as shown in the upper group of emission spectra observed with  $0.2 \text{ mW}$  average pumping power excitation in Figure 2. The photoluminescence (PL) spectra emitting from the un-patterned planar area of the same sample were shown in the lower group of emission spectra in Fig. 2. The inset in Fig. 2 presents temperature coefficients of both emission spectra from PC patterned and un-patterned area of the sample. Comparing with the rather large temperature-dependent PL shifting effect from un-patterned area of the sample ( $3.52 \text{ cm}^{-1}/\text{K}$  temperature coefficient), the emission peaks from PC patterned area were nearly independent on temperature with only  $0.16 \text{ cm}^{-1}/\text{K}$  temperature coefficient which is caused by the refractive index change under the temperature variation.<sup>7</sup> Similar to our previous report,<sup>6</sup> this phenomenon clearly indicates the optical coupling effect of the 2D PC cavity. However, the PC coupled emission peak does not match our designed theoretical emission wavelength ( $\sim 3.79 \mu\text{m}$ ). Comparing with the designed photonic band gap at around  $2640 \text{ cm}^{-1}$  ( $\sim 3.79 \mu\text{m}$ ) shown in Fig. 1, the PC coupled emission peak position blue shifts to  $2840 \text{ cm}^{-1}$  ( $\sim 3.52 \mu\text{m}$ ). To explain this phenomenon, we checked the dimension of the etched Si pattern and found that, for this particular sample, the radius of etched holes is  $1.14 \mu\text{m}$ , which is larger than the designed  $1.10 \mu\text{m}$ . Simulation using the actual  $1.14 \mu\text{m}$  radius shows a higher photonic band gap from  $2807$  to  $3063 \text{ cm}^{-1}$  which matches the experimental result. We noticed in Fig. 2 that under the condition of  $0.2 \text{ mW}$  average pumping power, the linewidths of the emission spectra at 300 K and below are significantly narrower than that at 310 K. This is because the pumping intensity applied was above lasing threshold of room temperature and below. The threshold behavior at 300 K will be discussed in the followings.

The characteristic of output light power versus input light power was measured at room temperature with input

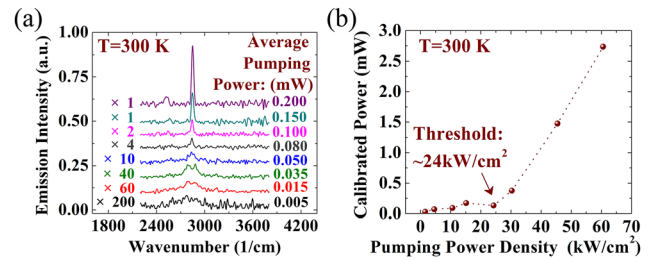


FIG. 3. (Color online) (a) PC coupled pulsed light emission spectra (resolution:  $16 \text{ cm}^{-1}$ ) with different pumping intensity at room temperature and (b) calibrated PC laser peak output power as a function of the peak pumping power density at 300 K.

average pumping powers from  $5 \mu\text{W}$  to  $0.2 \text{ mW}$ , as shown in Figure 3(a). As the pumping power becomes higher than  $0.08 \text{ mW}$ , significant linewidth narrowing effect starts to occur, and the intensity of the light emission increases dramatically with the pumping power. The peak output emission powers were calibrated by a standard blackbody reference source. Figure 3(b) shows the peak output power versus peak pumping power density (P-P) curve of the PC structure emission with a clear threshold behavior. The threshold peak pumping power density is  $\sim 24 \text{ kW}/\text{cm}^2$  at 300 K. Material quality improvement<sup>8</sup> and the group-velocity anomaly effect<sup>9</sup> ( $v_g$  is equal to zero) could have played important roles in lowering the threshold. But this value is still 30 times higher than the reported IV-VI surface-emitting microdisk laser by Eibelhuber *et al.*<sup>10</sup> whose threshold pumping density is  $0.76 \text{ kW}/\text{cm}^2$  at 273 K. However, in this work, the peak positions between PC mode and the QW gain, as shown in Fig. 2, have a big mismatch. We would expect a much lower threshold once they could match.

The analysis of the PC coupled far-field emission profiles above and below pumping threshold is presented in Figure 4. As is shown, Gaussian distribution fits well with the angular dependent emission profiles. When the PC-patterned area was under below-threshold optical excitation (average pumping power:  $0.015 \text{ mW}$ ), the PC coupled emission exhibited a broad far-field profile with full width at half maximum of  $\sim 29.7^\circ$ . This angular dependence is due to the high contrast of refractive index between  $\text{BaF}_2/\text{air}$  and lead-salt material and modification effects of PC-patterned structure.<sup>11</sup>

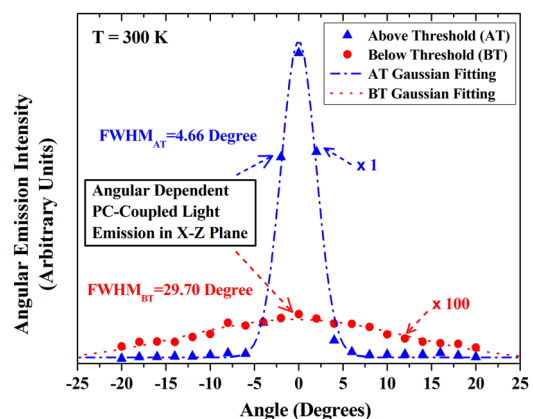


FIG. 4. (Color online) Angular dependence of the PC coupled emissions above threshold pumping (solid triangle) and below threshold pumping (solid circle); the curves are Gaussian fittings.

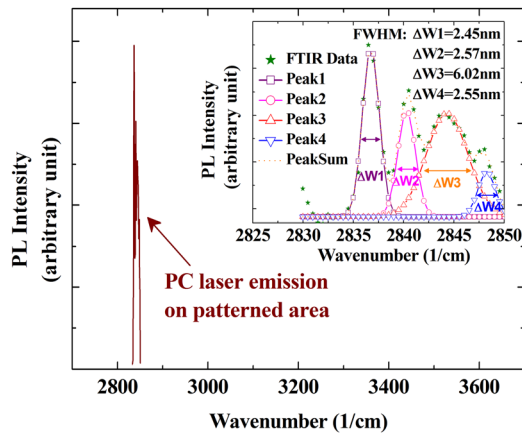


FIG. 5. (Color online) PC coupled laser emission spectrum (resolution:  $1\text{ cm}^{-1}$ ) at 300 K. Multi-mode lasing information and linewidth determined by Gaussian function fitting are presented in the inset.

However, with above-threshold pumping (average pumping power: 0.2 mW), the FWHM of the angular emission profile decreased significantly to  $4.66^\circ$ , indicating narrow lasing beam divergence. This performance is approaching to the reported  $3.46^\circ$  near diffraction limit beam quality achieved in the IV-VI vertical external cavity surface emitting lasers by Khiar *et al.*<sup>12</sup>

The laser emission spectrum at 300 K measured with  $1\text{ cm}^{-1}$  resolution reveals that the PC coupled emission includes multiple peaks as shown in Figure 5. Based on our design, those emission peaks are PC microcavity modes generated by the defect cavity in the center of PC array. However, we would like to point out that, there could be other mechanisms contributing to the multi-mode emission, such as degeneracy splitting of dipole mode<sup>13</sup> due to the structure imperfection and photonic band-edge mode emission.<sup>4</sup> Details of the multi-mode behavior need to be further studied. Using Gaussian function fitting, their FWHM were determined as shown in the inset of Fig. 5. The narrowest

linewidth is 2.45 nm (Q factor is 1437.68). This linewidth is relatively broad, which is similar to the reported microdisk IV-VI surface emitting laser.<sup>10</sup> This phenomenon is most likely caused by the roughness around etched circles by processing and overgrowth.

In conclusion, we have designed and experimentally realized an optically pumped mid-infrared surface-emitting photonic crystal laser on silicon substrate operating at room temperature. Multi-mode lasing emissions were observed at around  $3.5\ \mu\text{m}$ . With different QW thickness design, such RT PbSe/PbSrSe QW PC laser could cover wavelength range from  $4.5\ \mu\text{m}$  to  $3.3\ \mu\text{m}$ .

Funding was partially provided by the DoD ARO under Grant No. W911NF-07-1-0587, NSF Grant No. DMR-0520550, and by Oklahoma OCAST program under Grant Nos. AR112-18 and AR082-052.

- <sup>1</sup>H. Park, J. Hwang, J. Huh, H. Ryu, and Y. Lee, *Appl. Phys. Lett.* **79**, 3032 (2001).
- <sup>2</sup>M. Loncar, T. Yoshie, A. Scherer, P. Gogna, and Y. Qiu, *Appl. Phys. Lett.* **81**, 2680 (2002).
- <sup>3</sup>H. Altug, D. Englund, and J. Vuckovic, *Nat. Phys.* **2**, 484 (2006).
- <sup>4</sup>R. Colombelli, K. Srinivasan, M. Troccoli, O. Painter, C. F. Gmachl, D. M. Tennant, A. M. Sergent, D. L. Sivco, A. Y. Cho, and F. Capasso, *Science* **302**, 1374 (2003).
- <sup>5</sup>M. Kim, C. S. Kim, W. W. Bewley, J. R. Lindle, C. L. Canedy, I. Vurgaftman, and J. R. Meyer, *Appl. Phys. Lett.* **88**, 191105 (2006).
- <sup>6</sup>B. Weng, J. Ma, L. Wei, J. Xu, G. Bi, and Z. Shi, *Appl. Phys. Lett.* **97**, 231103 (2010).
- <sup>7</sup>A. Majumdar, H. Z. Xu, F. Zhao, J. C. Keay, L. Jayasinghe, S. Khosravani, X. Lu, V. Kelkar, and Z. Shi, *J. Appl. Phys.* **95**, 939 (2004).
- <sup>8</sup>B. Weng, F. Zhao, J. Ma, G. Yu, J. Xu, and Z. Shi, *Appl. Phys. Lett.* **96**, 251911 (2010).
- <sup>9</sup>K. Sakoda, *Optical Properties of Photonic Crystals* (Springer, New York, 2001).
- <sup>10</sup>M. Eibelhuber, T. Schwarzl, S. Pichler, W. Heiss, and G. Springholz, *Appl. Phys. Lett.* **97**, 061103 (2010).
- <sup>11</sup>S. H. Kim, S. K. Kim, and Y. H. Lee, *Phys. Rev. B* **73**, 235117 (2006).
- <sup>12</sup>A. Khiar, M. Rahim, M. Fill, F. Felder, F. Hobrecher, and H. Zogg, *Appl. Phys. Lett.* **97**, 151104 (2010).
- <sup>13</sup>O. Painter, J. Vuckovic, and A. Scherer, *J. Opt. Soc. Am. B* **16**, 275 (1999).